

Dr. Fermín Huarte Larrañaga  
*Departament de Ciències Materials i  
Química Física*

Dr. Ricardo Molina Mansilla  
*Institut de Química Avançada de Catalunya  
(IQAC-CSIC)*



# Treball Final de Grau

**Modulation of seed germination by plasma surface treatments.**

**Modulació de la germinació de la llavor per tractaments  
superficials de plasma.**

Alba Lalueza Sánchez

*June 2019*



UNIVERSITAT DE  
BARCELONA

**B·KC** Barcelona  
Knowledge  
Campus  
Campus d'Excel·lència Internacional



Aquesta obra esta subjecta a la llicència de:  
Reconeixement–NoComercial-SenseObraDerivada



<http://creativecommons.org/licenses/by-nc-nd/3.0/es/>



Gràcies, de tot cor, als meus tutors, els doctors Ricardo Molina Mansilla i Fermín Hurte Larrañaga. Gràcies per la seva paciència, dedicació, motivació, criteri i experiència. Ha sigut un plaer poder tenir la seva ajuda.

Gràcies a totes les persones que, d'alguna manera o d'un altre, han sigut claus durant tot el grau. Però per sobretot, a la meua família i amics, que han estat sempre incondicionalment al meu costat.



**REPORT**





# CONTENTS

<b>1. SUMMARY</b>	3
<b>2. RESUM</b>	5
<b>3. INTRODUCTION</b>	7
3.1. What is plasma?	7
3.1.1. Plasma classification	8
3.1.2. Cold plasma technology	9
3.1.2.1. Discharge at atmospheric pressure	10
3.2. Chemistry of plasma	10
3.2.1. Cold plasma for superficial treatments	11
3.2.1.1. Surface erosion	11
3.2.1.2. Surface functionalization	12
3.2.2. Plasma characterization	12
3.3. Plasma in agriculture	13
3.3.1. Structure and composition of wheat seeds	13
3.3.2. Surface characterization of seed	15
3.3.2.1. Contact angle	15
3.3.2.2. Scanning Electron Microscopy	16
3.3.2.3. Fourier-Transform Infrared Spectroscopy coupled to Attenuated Total Reflectance	16
3.3.2.4. X-ray Photoelectron Spectroscopy	17
<b>4. OBJECTIVES</b>	19
<b>5. EXPERIMENTAL SECTION</b>	19
5.1. Atmospheric cold plasma treatment	19
5.2. Materials and germination conditions	20
<b>6. STUDY OF PLASMA CHEMICAL SPECIES</b>	23
<b>7. GERMINATION AND ABSORPTION RESULTS</b>	24

---

<b>8. SURFACE CHARACTERIZATION OF SEEDS</b>	27
<b>9. FUTURE WORKS</b>	32
<b>10. CONCLUSIONS</b>	33
<b>11. REFERENCES AND NOTES</b>	35
<b>APPENDICES</b>	37
Appendix 1: OES	39
Appendix 2: FTIR-ATR	40

# 1. SUMMARY

In this study the modulation of the surface properties of wheat seeds is studied, such as hydrophilicity, promoted by the effect of plasma. Thanks to the improvement in the kinetics of the water uptake, we can improve the efficiency in the germination process during short treatment times (< 120 s). While long times treatment and wet conditions has seen relented germination (> 300 s). This fact has been attributed to the fact that key processes in the germination such as the exchange of gases ( $O_2$  and  $CO_2$ ), it is hampered by the accumulation of water in the outer layers of the seed. Total germination is equal to all times of treatment, which has allowed to reject the possibly damage to the embryo. On the other hand, they have characterized the physicochemical changes induced by the plasma in the surface seeds. The OES has determined the chemical species present in the plasma, among which are oxidant species such as hydroxyl radicals and monoatomic radicals of oxygen. Based on the techniques of XPS, SEM and FTIR-ATR has determined the presence of a nanometric layer that covers pericarp (matrix of lignocellulose), with more than 90% of links C-C and/or C-H, that when they oxide (incorporation of polar groups) reverses the polarity of the layer making the surface more hydrophilic. Starting from 300 s treatment, all the techniques used suggest a plasma-induced etching effect that degrades totally or partially the outer layer of wheat seeds.

**Keywords:** Plasma, hydrophilicity, germination, wheat, etching, OES, FTIR-ATR, XPS, SEM.



## 2. RESUM

En aquest treball s'estudia la modulació de les propietats superficials de les llavors de blat, com la hidrofília, promoguda per l'efecte del plasma. Gràcies a la millora en la cinètica de la captació d'aigua, podem millorar l'eficiència en el procés de germinació a curts temps de tractament (< 120 s). Mentre que a temps llargs de tractament i de condicions humides s'ha vist alentitzada la seva germinació (> 300 s). Aquest fet s'ha atribuït al fet que processos clau en la germinació com l'intercanvi de gasos ( $O_2$  i  $CO_2$ ), es veu obstaculitzat per l'acumulació d'aigua a les capes exteriors de la llavor. La germinació total s'igualava per a tots els temps de tractament, el que ha permès descartar possibles lesions a l'embrió. D'altra banda, s'han caracteritzat els canvis fisicoquímics induïts pel plasma en la superfície de les llavors. Amb l'OES s'ha determinat les espècies químiques presents en el plasma, entre les quals es troben espècies oxidants com els radicals hidroxils i els radicals monoatòmics d'oxigen. A partir de les tècniques de XPS, SEM i FTIR-ATR s'ha determinat la presència d'una capa nanomètrica que cobreix el pericarpí (matriu de lignocel·lulosa), amb més del 90% d'enllaços C-C i/o C-H, que quan s'oxiden (incorporació de grups polars) reverteix la polaritat de la capa fent que la superfície sigui més hidròfila. A partir dels 300 s de tractament, totes les tècniques utilitzades suggereixen un efecte d'etching induït pel plasma que degrada totalment o parcialment la capa exterior de les llavors de blat.

**Paraules clau:** plasma, hidrofília, germinació, blat, etching, OES, FTIR-ATR, XPS, SEM.



## 3. INTRODUCTION

Plasma technology has now developed rapidly in many sectors of modern industry such as the aerospace industry, microelectronics, automotive, etc. This is due to the fact that the plasma is able to modify the surface properties of materials to improve their applications without change the bulk properties. The way in which the plasma interact with all surfaces is unknown in detail, but certain mechanisms of modification, such as deposition, erosion or the functionalization of surfaces are known. They can happen at the same time or separately.<sup>1</sup>

### 3.1. WHAT IS PLASMA?

Plasma is the fourth state of matter and it constitutes 99% of the known matter so far.<sup>2</sup> Instead, it is unusual in our day to day because its formation requires energy conditions (pressure and temperature), which are more common in space. This energy can be thermal or electrical type. The last one can be used to produce plasma in the laboratory by electric discharges to gases. Due to the contribution of energy, collisions occur between the particles that led to the ionization of the gas.

A plasma substance is an ionized gas in which some or all atoms that compose it has lost and won electrons, constituting free species electrically charged. The plasma is formed with the same number of positive and negative charges, resulting in a quasi-neutral system.<sup>3</sup> For this reason, we discuss another state of matter because it has different properties to gas, such as the electrical conductivity and a great reaction to the magnetic field. The term “plasma” for an ionized gas was introduced in 1927, for the first time by Irving Langmuir.<sup>4</sup>

The plasma is constituted by electrically charged particles, such as ions and electrons, very reactive neutral species, such as free radicals or atoms, excited molecules, excimers<sup>5</sup> and monomers. (Figure 1) It is a very reactive state in which molecules are broken releasing atoms and radicals that react chemically and quickly forming new species.

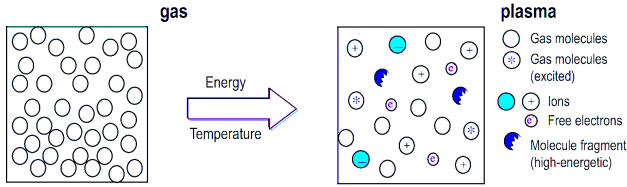


Figure 1. Schematic view of plasma with freely moving charges.

Also, a plasma could return to a gaseous state by a de-ionization process. The light emitted by the plasma is due to the processes of de-excitation of the atoms, molecules and ions that constitute it. This characteristic emission for each species emits electromagnetic radiation, which can be visible or not.

Some examples of plasma that may exist in the universe are the solar crown, the solar wind, the Earth's ionosphere and the nebulae. You can also find terrestrial examples such as Aurora borealis, lightning, fire, fluorescent lamps and also plasma television.

### 3.1.1. Plasma classification

The most important parameters of plasmas are their free electric charge density ( $n_e$ ) and their electronic temperature ( $T_e$ ). These allow to classify the plasmas according to their heavy particles energy or, in other words, according if they are or are not in thermodynamic equilibrium. There are two types of plasmas. One of them is in thermodynamic equilibrium called thermal plasmas ( $T_e = T_{\text{gas}}$ ). And the other that is not in thermodynamic equilibrium, it is called cold or non-thermal plasmas, which is usual in low pressures. ( $T_e \neq T_{\text{gas}}$ ).

The thermal plasmas have a temperature of  $10^3$ - $10^4$  K. Its main characteristics are to have a high free electron density ( $10^{20}$ - $10^{25}$  electrons·m<sup>-3</sup>)<sup>6</sup>. The gas temperature is much higher than the melting point of the most materials, so it is practically impossible to make superficial treatments without damaging the sample. That is why, thermal plasmas only are used as a source of energy.

The cold or non-thermal plasmas have an electronic temperature of  $10^5$  K, while the other particles, which are not in thermal equilibrium, are at room temperature. This type of plasma is found in low-energy lamps, and is used for the production of thin films and surface treatments. This one allows reactions that could not be given at such high temperatures. Also, the proportion



of molecules is greater than ions and radicals because their degree ionization is lower. As a result, is what confers that high chemical reactivity at low temperature. These plasmas have a high free electrons density, but less than in thermal, and the temperature is very lower, about  $10^2$  K that is close to room temperature.<sup>7</sup>

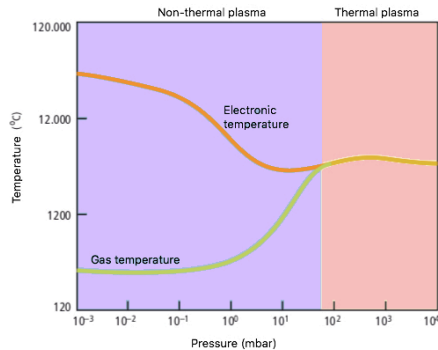


Figure 2. Thermal and non-thermal plasma

### 3.1.2. Cold plasma technology

In current plasma technology based on the industry and science research, the cold plasma, or as described above, the plasma in a non-thermal equilibrium is used. It allows surface treatments because it is possible to have a high electronic energy at low temperature. And this is an essential factor to initiate many of the chemical reactions efficiently unlike other thermally ordinary processes. These plasmas can generate many reactive species that could start physical and chemical processes, in a cheaper and more environmentally friendly way.

In low pressures, the working voltage is usually around 1 kV for a power of 100 W<sup>7</sup>. First, the vacuum is performed and then the gas is injected continuously. Once it remains in the desired pressure, the gas is ionized by direct current, radio frequency or microwave. The advantages of working at low pressure are that the process is very controlled and it is environmentally friendly. Besides, it requires a little amount of chemicals and that plasma production can be done in a short time. One of the most important drawbacks is that the cost because it requires a vacuum system and the complicated application in an industry chain, i.e. in a continuous production, too.

In the atmospheric pressure plasma, the equipment that produces it does not require a vacuum system. Thus, the cost is cheaper and it can also be incorporated into a manufacturing

chain. This technique also allows to treat more delicate samples that can be damaged by vacuum. With regard to vacuum plasma there are certain disadvantages, such as the generation of ozone if the plasma contains oxygen.<sup>8</sup> Another inconvenient is that the process is not as controlled as in vacuum.

### *3.1.2.1. Discharge at atmospheric pressure*

The plasmas can be differentiated according to the frequency of excitation that is applied, which can be direct current at low frequencies of discharge (1 MHz), radio frequency (1 MHz to 1 GHz) and microwave discharges in which the frequencies are above 1 GHz. Also, we can differentiate these plasmas depending on the way they are produced. They are called corona discharge, dielectric barrier discharge (DBD) and incandescent or glow discharge. In this work will focus on surface treatments by plasma DBD, because it is the most suitable application to get as homogeneously as possible the seeds atmospheric pressure.<sup>9</sup>

## **3.2. CHEMISTRY OF PLASMA**

The most important process is the initial ionization that precedes the formation of the plasma. Then, electrons are accelerated by applied external electromagnetic fields and they gain energy. In this way, they have more kinetic energy and collide with atoms and neutral species, producing an ionization in chain. The degree of ionization depends on the species that compose the plasma and gives rise to plasmas of different characteristics (oxidant or reducer). When the ionization is low there is a strong thermal imbalance because the energy is barely transferred between electrons and heavy particles. When you stop supplying power, the plasma shuts down, almost immediately.

Also other processes are given in the meantime as atomic excitation, which is caused by the electronic impact with electron of characteristics energies. In addition, occurs the de-excitation, the plasma emits photons of discrete and determined energies. The molecular dissociation is given, too. To sum up, the plasmas are a reactive medium in with the molecules become in radicals or in excited species and interact with each other to form new chemical products.

### 3.2.1. Cold plasma technology

There are different mechanisms in which the plasma interacts with the surface. According to the average energy of the free electrons (1-10 eV) and the type ionized gas, the plasma will induce a different plasma-surface interaction, such as, deposition, erosion and functionalization. It should be noted that the superficial modification is only a few nanometers, leaving the most internal properties of the material intact. Currently, the most plasma treatments are based on improving de wettability and bonding with the surface of the materials.<sup>11</sup> Also, they can allow to create a few available bonding sites, to get low surface energies and be more hydrophobic and for decontamination of surfaces. The success of these processes is due to the various advantages it has with respect to the conventional chemical and physical processes. For example, the low consumption of chemicals, which is environmentally friendly, allows to treat thermal sensitive samples, gets highly reactive species, short treatment times. In addition, it allows surface modification without altering bulk properties.

#### 3.2.1.1. Surface erosion

Erosion is the assisted wear caused by the ionic bombardments that promote the plasma to the surface. There are two methods called etching<sup>12</sup> and sputtering<sup>13</sup>. On the one hand, etching is the chemical mechanism in which the plasma species bombard the surface reacting with the outermost atoms. Giving rise to volatile products that escape from surface material. (Figure 3) On the other hand, sputtering is the physical mechanism that the reactive species of plasma collision with the atoms of the surface very energetically. And expel them from the matrix granting a part of their kinetic energy. (Figure 4)

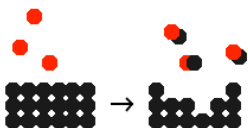


Figure 3. Schematic view of etching mechanism.

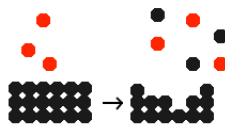


Figure 4. Schematic view of sputtering mechanism.

Argon and helium are used for inert cleaning because only is a physic process by energetic electron bombardment. Always oxygen plasma is very effective in remove organic compounds,

such as lipids, oxidizing the hydrocarbon chain and releasing CO<sub>2</sub>.<sup>14</sup> And hydrogen plasma is used to eliminate oxides, thanks to the reductive properties.

### 3.2.1.2. Surface functionalization

Many materials have a too inert or non-wettable surface. The activation of the surface is a solution and consists in the creation of places with radicals in which it makes it more reactive. For example, argon and helium plasma remove individual atom from the surface by impact. The radicals that remain free form highly reactive spaces and favor the union with other compounds. Also, oxygen plasma completely inverts the polarity of the material, transforming its surface into more wettable. It generates hydroxyl groups, carbonyls and esters.<sup>14</sup>

### 3.2.2. Plasma characterization

To characterize the reactive chemical species that induce the plasma, the spectroscopic technique known as Optical Emission Spectroscopy (OES) is used. The emission of electromagnetic radiation of the previously excited species that constitute the plasma occurs, the difference of energies is emitted as a photon and its energy is detected. Each level of energy is defined by its electronic, vibrational and rotational energy, and as a consequence of each transition, is associated with a wavelength in a characteristic frequency. The space of the energy between the vibrational and rotational states is much smaller than between the electronic states which are in the UV-Vis zone (300-850 nm).<sup>15</sup> Only permitted transitions which conserved the angular momentum and emissions in that wavelength range can be characterized. It should be noted that there could be other transitions that do not emit or emit in other range although they cannot be detected with this microscopy. Therefore, they are part of the plasma.

The reactive species and their amount depend on the type of gas, the humidity, the frequency, the voltage and the intensity of the electric current that is applied to it. There are two main groups of very reactive species that in the presence of air plasma, are formed. These are the reactive oxygen species (ROS) and the reactive nitrogen species (RNS)<sup>16</sup>. The creation of these is given by the interaction with the air and water vapour, and give rise to species such as free radicals (NO·, OH·, superoxide O<sub>2</sub><sup>·-</sup>) and strongly oxidizing agents (H<sub>2</sub>O<sub>2</sub> y O<sub>3</sub>). Excited states of O<sub>2</sub> and N<sub>2</sub> can also be formed by energy absorption. The presence of monoatomic oxygen (<sup>3</sup>P, fundamental state), can indicate the presence of other of its excited states (<sup>1</sup>D and <sup>1</sup>S) although its multiplicity changes and therefore its transition is forbidden. Above all the state with the electronic term, <sup>1</sup>D

is known to be very electrophilic to have a free orbital.<sup>17</sup> (Figure 5) These species are very unstable; they have a half-life of nanoseconds because they are recombined forming other compounds very quickly.

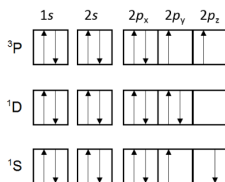


Figure 5. Fundamental state of atomic oxygen (<sup>3</sup>P), first excitation state is (<sup>1</sup>D) and the second excitation state is (<sup>1</sup>S).

### 3.3. PLASMA IN AGRICULTURE

The plasma applied to agriculture is, for the moment, a very unknown area. The modification of the surface of the seeds to increase their hydrophilicity is a mechanism that is not yet known in detail, and will be studied in this project. It is only known that it improves the absorption of water that is related to germination. Other applications of plasma technology in agriculture, are the activation of water, increasing the content of nitrogen compounds, post-germination treatments, for higher plant growth.<sup>18</sup> And finally, also for humid areas, to increase the hydrophobia of the outer layer of the seed with the presence of fluorinated compounds in the plasma.<sup>19</sup>

Currently, there are pre-germinative methods to break the latency of a seed, which is the inability of a seed germinate although apparently the conditions are suitable. One of the methods is stratification, which consists of cooling the seeds to break the physiological latency of the seed. Another is the scarification process that is to crack the external coat of the seed, the disadvantage is that many of the seeds are damaged during the process. And finally, the chemical scarification, which consists of soaking the seeds for a short period of time in H<sub>2</sub>SO<sub>4</sub>.

#### 3.3.1. Structure and composition of wheat seeds

In this project, it has been chosen the wheat seed because its germination is very fast. The seed is covered by pericarp, composed by outer pericarp and inner pericarp with the same compounds, but in different amounts. The composition is cellulose, hemicellulose, such as,

arabinoxylans and lignin.<sup>21</sup>(Table 1) Also, these layers have phenolic compounds, too. Other inner layers there are in the pericarp (testa, hyaline layer and aleurone). These layers protect the endosperm and the embryo. The endosperm constitutes the 85% of grain weight and it contains the reserves for the development of the embryo. And finally, the germ consists of the embryonic axis and the scutellum that functions as a storage organ. With surface treatments by cold plasma only modify a few nanometers with which only would be observed changes in the outer pericarp. It should be noted that pericarp could be contains fat and waxy substances that provides impermeability to the seed.<sup>22</sup>

Composition	% Pericarp
Hemicellulose	60
Cellulose	25
Lignin	12
Phenolic compounds	0,5
Others	2,5

Table 1. Composition of pericarp in the wheat seeds.<sup>22</sup>

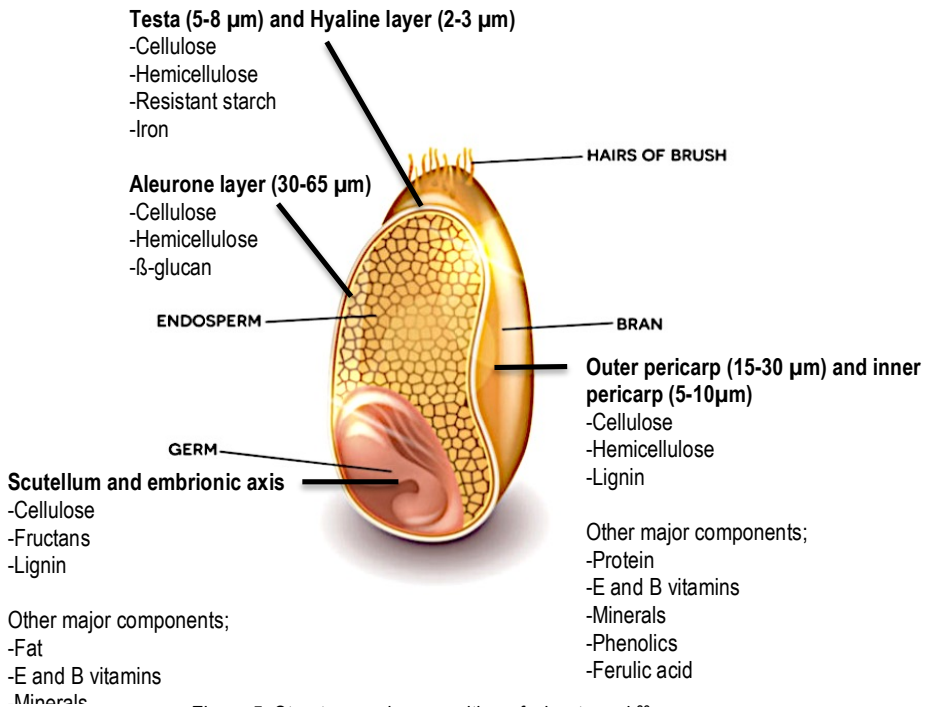


Figure 5. Structure and composition of wheat seed.<sup>23</sup>

### 3.3.2. Surface characterization of seed

To know the different depth sensitivities of each technique used are very important to the correctly characterization the plasma-surface interaction. (Table 2)

Technique	Depth sensitivity (nm)
FTIR-ATR	500-1500
XPS	5-10
SEM	~1000
Contact angle	Until 0,5

Table 2. Depth sensitivity for each technique used.<sup>24</sup>

#### 3.3.2.1. Contact angle

The contact angle is a parameter used in materials to characterize the wettability properties of these. It refers to the angle that the surface of a liquid forms when coming into contact with a solid. The value of the contact angle depends mainly on the relationship between the adhesive forces and the cohesive forces of the liquid.<sup>25</sup> When the adhesive forces with the surface of the solid are very large in relation to the cohesive forces, the contact angle is less than 90 degrees, resulting in the liquid wetting the surface. Therefore, in a qualitative way because the seed is not a planar surface, if the contact angle is greater than 90°, it will be considered a hydrophobic seed surface. On the other hand, for a contact angle lower than 90°, the surface has been modified so that it is more hydrophilic and wettable.

$$0 = \gamma_{SG} - \gamma_{SL} - \gamma_{LG} \cos \theta_c$$

Equation 1. Young equation.  $\gamma_{SG}$  is the intersuperficial energy solid-vapor,  $\gamma_{SL}$  is the intersuperficial energy solid-liquid,  $\gamma_{LG}$  is the surface tension liquid-vapor and  $\theta_c$  is the contact angle in equilibrium.<sup>25</sup>

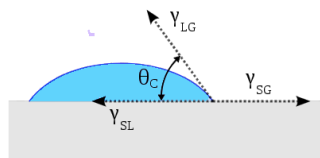


Figure 6. Example of contact angle.

### 3.3.2.2. Scanning Electron Microscopy

Scanning Electron Microscopy (SEM) is based on the targeting of a high-energy electron beam on the sample, scanning its surface. The image is obtained as a result of the interaction of these electrons with the substrate. It can interact in an elastic or inelastic way. In the elastic interaction modifies the direction of the electrons incidents without the energy kinetic change and allows the lateral resolution of the microscope the detection of these, called retrodiffused electrons. In the inelastic interaction, electron loses a part of the kinetic energy that is passed to the atoms of the surface without affecting the trajectory that it had. This phenomenon is responsible for the in-depth resolution and the generation of X-rays, Auger electrons, and secondary electrons.<sup>26</sup> The detection of the latter is those that allow to characterize the topography of the seed. The sample must be electric conductive or with a nanometric metallic coating, like gold, so that the surface is not charged and affects the trajectory of the secondary electron.

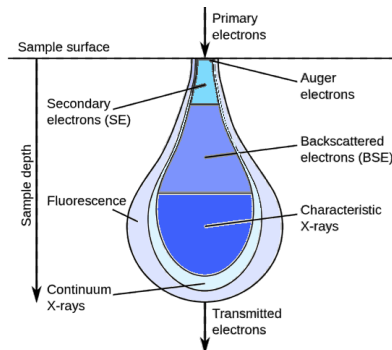


Figure 7. Scheme of Scanning Electron Microscopy.

### 3.3.2.3. Fourier-Transform Infrared Spectroscopy coupled to Attenuated Total Reflectance

The FTIR-ATR is a technique that allows us to characterize a few micrometers of depth in the seed. As the superficial modification induces of the plasma could not be observed. Since it is under the depth limit of the detection. Even so, it allows knowing the chemical composition of the layers. The technique is based on absorption spectroscopy, in which a beam of infrared radiation interacts with the sample. This beam suffers multiple reflections inside crystal (diamond) and some of its energy is lost because it penetrates the sample.



ATR's complement is based on measuring the changes occurring in the infrared beam when it comes into contact with a refraction index crystal or a large angle of incidence. The reflectance provokes an evanescent wave that extends through the surface of the glass and having contact with the surface of the seed. At more angle of incidence, more index of refraction of the glass and lower wavelength of the infrared beam, it will be possible to characterize functional groups that are in the outermost layers.<sup>27</sup>

$$d = \frac{\lambda}{2\pi n_1 \sqrt{\sin^2 \theta - n_{21}^2}} ; n_{21} = \frac{n_2}{n_1}$$

Equation 2.  $d$  is the depth of the evanescent wave penetration,  $\lambda$  is the wavelength of beam,  $n_1$  refraction index of crystal,  $n_2$  is the refraction index of substrate and  $\theta$  is the incident angle of infrared beam.<sup>27</sup>

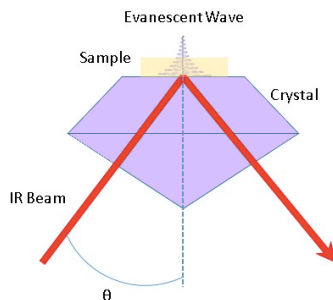


Figure 8. Scheme of Attenuated Total Reflectance

#### 3.3.2.4. X-ray Photoelectron Spectroscopy

The technique of X-ray Photoelectron Spectroscopy (XPS) can provide qualitative and quantitative information of all the elements present, except H and He. It consists of irradiating the sample with a monoenergetic X-ray beam and detecting the electrons emitted by the surface by the photoelectric effect. The kinetic energy with which the electron is detected after photon absorption by atom is described with the following equation.<sup>28</sup>

$$E_{kin} = h\nu - E_B - \phi_{spec}$$

Equation 3.  $E_{kin}$  is the photoelectron kinetic energy,  $h\nu$  is the incident radiation energy,  $E_B$  is the binding energy and  $\phi_{spec}$  is the spectrometer work function.

The variable, working function  $\phi_{spec}$ , is the extra energy needed to remove the electron from the surface. As a source of X-rays, a sample of Mg K $\alpha$  (1253,6 eV) or Al K $\alpha$  (1486,6 eV) is used, which is bombarded by electrons, producing an ionization. Consequently, the emission of X-rays.<sup>28</sup>

It should be taken into account that the more internal the electron the stronger it will be its binding energy. This energy will also vary depending on the type of atom to which one can alter the electronic distribution. The case of the isotopes, they have different number of electrons, but equal nuclear load therefore the binding energy will not change. Neither the hydrogen bonds nor the crystallizing forces alter the electronic distribution as to modify the binding energy that is measured. It produces a phenomenon called Chemical Shift<sup>28</sup>, which is that the most external electrons to participate in the links cause the atom to lose negative charge and the internal electron is more attracted by the nucleus.

Auger electron emission may occur<sup>28</sup>. These unlike photo electrons are independent of the energy of the incident photon beam. (Figure 10)

In the dielectric materials the expulsion of electrons gives rise to a superficial load and consequently to an electric field that decreases the  $E_{kin}$  and produces the bleed of the peaks in the spectrum. It is necessary to adjust manually and the difference of load is subtracted to all the peaks selecting as reference the peak C<sub>1s</sub> in which its energy of binding is 285.0 eV.<sup>28</sup>

The superficial sensitivity is given by the following equation.

$$d = 3\lambda \cos\alpha$$

Equation 4.  $d$  is the depth resolution  $\lambda$  is the travel of free electrons and  $\alpha$  is the detection angle.<sup>28</sup>

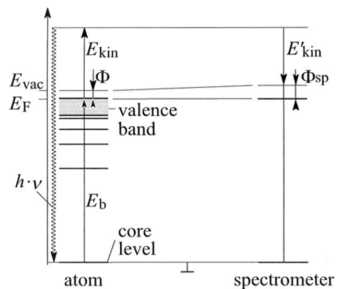


Figure 9. Schematic of XPS principle.

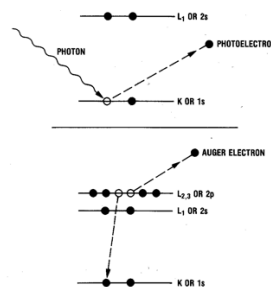


Figure 10. Photoelectron and Auger electron.

## **4. OBJECTIVES**

The project focuses on the superficial modification of wheat seeds by DBD plasma in order to modify their hydrophilicity, altering the kinetics of water absorption and in this way modulate their germination.

Another main objective is to relate the observed changes in the germination process with the physicochemical changes on the seed surface induced by plasma. It is required to characterize the plasma to know the chemical species involved in the superficial modification and characterize the topography, contact angle and the chemical composition of the outers layers of seed.

## **5. EXPERIMENTAL SECTION**

This section describes the experimental procedures and the characterization techniques to study the morphological and chemical modification that has had induce by the dielectric barrier discharges.

### **5.1. ATMOSPHERIC COLD PLASMA TREATMENT**

The atmospheric plasma used was generated in a dielectric barrier discharge reactor (DBD), a type of atmospheric cold plasma treatment, consisting of two superimposed simple beakers with an interspace. (Figure 11) It was formed by two parallel metal electrodes (45 mm in diameter separated by 12 mm and covered by glass that acts as a dielectric plate. To avoid discharge arcs that could damage the surface coating of the seed or that could do a heterogeneous treat. Helium was used as the primary plasma gas because its dielectric break is 0.15 kV/mm, lower than the air 0.4 kV/mm. Its flow (5 L/min) was controlled with a mass flow meter and controller (Bronkhorst, Ruurlo, Netherlands). A 16 kHz signal was generated with a Function Generator GF-855 (Promax,

L'Hospitalet de Llobregat, Spain) connected to a line at amplifier AG-1012 (T & C Power Conversion, Inc., Rochester, NY, USA. UU.). A matching network and two transformers (HR-Diemen S.A., Sant Hipòlit de Voltregà, Spain) were connected to the output of the amplifier to increase the voltage up to 20kV. The wheat seeds were placed in the lower glass covering completely the electrode area, the incident power was adjusted to 30 W and the exposure time changed from 10 s to 900 s.

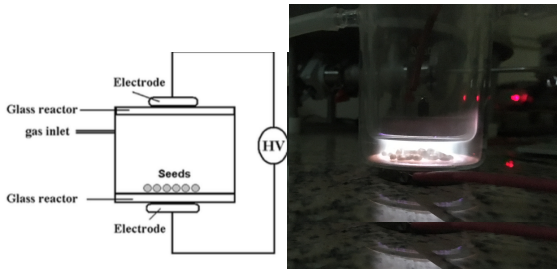


Figure 11. Dielectric barrier discharge reactor (DBD). Plasma of He and air impurities.

Optical emission spectroscopy (OES) was used to characterize the plasma system used. Diagnosis of the plasma gas was carried out with a quartz optic fiber spectrometer Black Comer (Stellarnet, Spain) with concave gratings. Spectra were recorded in UV-Vis wavelength range 190-850 nm with an integration time of 4 s. No UV emission was measured below 300 nm because the DBD reactor is made of borosilicate glass that cut off the wavelength there. Subsequently, CO<sub>2</sub>, N<sub>2</sub> and water plasmas were made to observe characterize some peaks.

## 5.2. MATERIALS AND GERMINATION CONDITIONS

The ecological seeds of wheat (*Triticum aestivum* L.) were obtained from Mapryser S.L. (Barcelona) and its certificate of origin is NL-BIO-01. The seeds were stored avoiding exposure to light and moisture. To carry out the treatment, the seeds that did not seem to have apparent damage were chosen. Weigh approximately 2,5 g of seeds by balance (KERN ABJ-NM/ABS-N), this weight allows covering the entire area that of electrodes for a homogeneous treatment as possible. Once the plasma application is finished, they are weighed again to study the weight loss. The process is repeated for different times of treatments, 10 s, 30 s, 60 s, 120 s, 300 s, 900

s, and six replicas are made for each time. The treated samples are stored in a desiccator at a RH of 53% at 25°C.

$$\% \textit{Weight loss} = \frac{W_{\textit{initial}} - W_{\textit{final}}}{W_{\textit{initial}}} \times 100$$

Equation 5. Percentage of seed weight loss after plasma

The simulation in the laboratory of the germination of the cereal consists of 55 seeds in each petri dish with four layers of filter paper (~ 1,25 g). The dishes remain dark, to avoid the differences of light between the different days of sowing and aired, but covered to avoid contamination in the samples. The germinated seeds are counted every 20 h, 24 h, 48 h and 72 h. It is considered that the seed has germinated when it is observed that the white radicle has emerged more than 1 mm. Germination is studied for three types of irrigation with ionized water, considered dry, optimal and wet conditions in previous qualitative experiments with untreated samples. The chosen irrigation conditions were 3 ml, 6 ml and 12 ml, respectively.

$$\% \textit{Germination rate} = \frac{N_{\textit{germinated seeds}}}{N_{\textit{total seeds}}} \times 100$$

Equation 6. Percentage of seed germination rate.

To study the water absorption, the preparation of the samples and the seeding is carried out in the same way. The water absorption is calculated by the weight gain in 1 h, 2 h, 4 h, 24 h and 48 h after watering. The temperature in the laboratory during the absorption is 21°C. When the germination begins and the radicle is observed, the data obtained are not true because the increase in weight does not correspond to the amount imbibition, but it is the growth of the plant.

$$\% \textit{Absorption} = \frac{W_{\textit{final}} - W_{\textit{initial}}}{W_{\textit{final}}} \times 100$$

Equation 7. Percentage of absorption.

To characterize the wettability of the seed surface as function the plasma treatment, the contact angle is qualitatively observed. It should be noted that the roughness factor of each seed affects the contact area, increasing wettability. A small drop of approximately 2 µL is deposited from a 0,5 µM dissolution of methylene blue (Certified by the Biological Stain Commission, Sigma-

Aldrich) in order to give the drop color and to appreciate better. The surface tension of methylene blue solutions at the micromolar level ( $\approx 71,0$  mN/m) is practically equal to that of de-ionized water ( $\approx 72,0$  mN/m).<sup>25</sup> The angle was calculated with a goniometer online (Goniometer PRO).

In order to characterize the chemical composition of the seeds, they are analyzed with the ATR-FTIR technique. The samples were taken out in a Nicolet AVATAR 360 spectrometer equipped with a Smart iTR ATR sampling accessory (Thermo Scientific, USA) in the range of 400-4000  $\text{cm}^{-1}$ . Measurements were performed using the Smart ATR Attenuated Total Reflectance (ATR) Sampling Accessory (Thermo Scientific INC, U.S.A). Spectra were obtained with an average of 32 scans using a resolution of 4  $\text{cm}^{-1}$ . An advanced ATR correction algorithm (OMNIC 7.3 from Thermo Electron Corporation) was used to correct for distortion intensity, peak shifts and polarization effects. Corrected ATR spectra were normalized (OriginPro 8.5.0) and correspond to the average of five samples.

Then, the surface chemical composition determined by XPS, too. The untreated and plasma modified seeds was analyzed using a PHI 5000 Versaprobe II XPS device equipped with an Al K $\alpha$  X-ray source ( $h\nu = 1486.6$  eV)<sup>28</sup> operated at 25 W. All measurements were conducted in a vacuum of at least  $10^{-6}$  Pa and the photoelectrons were detected with a hemispherical analyzer positioned at an angle of  $45^\circ$  with respect to the normal of the sample surface. Survey scans and individual high resolution C $_{1s}$ , O $_{1s}$  and N $_{1s}$  spectra were recorded with a pass energy of 187.85 eV (eV step = 0.8 eV) and 23.5 eV (eV step = 0.1 eV) respectively. Binding energies were referenced to the C $_{1s}$  photoelectron peak position for C-C and C-H species at 285.0 eV<sup>28</sup>. Surface composition was estimated after a linear background subtraction from the area of the different photoemission peaks modified by the corresponding sensitivity factors.

To observe the morphology of untreated and plasma treated seeds was assessed by Scanning Electron Microscopy with an acceleration voltage of 5 kV (HITACHI S-4800, from ICM-CSIC). Prior to SEM imaging, a Quorum Q150RS gold sputter coater was used to deposit a gold coating of a thickness of approximately 20 nm on the seeds to minimize charging. Different pictures of the pericarp were taken on both sides, at 500, 1000, 10000 and 20000 magnifications.

## 6. STUDY OF PLASMA CHEMICAL SPECIES

Optical emission spectroscopy is used to study the chemical species that form the plasma. It allows to characterize species whose de-excitation emit radiation with a wavelength between 300-850 nm.

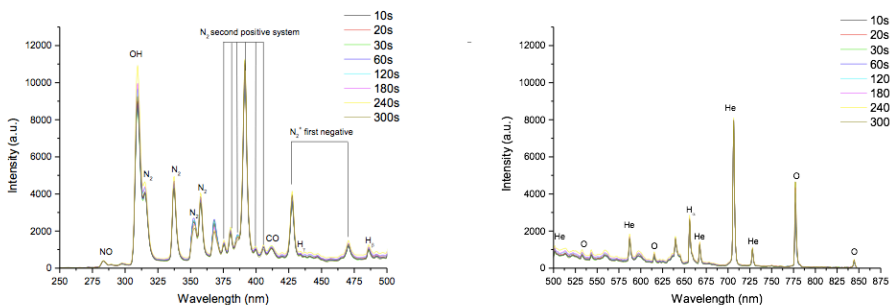


Figure 12. Optical Emission Spectroscopy spectrum of the He/air plasma.

In the spectrum, gives information about the existence of air impurities in the He plasma, such as, monoxide of nitrogen, hydroxides, exited nitrogen (SPS and FNS), hydrogen, monoatomic oxygen and helium. (Figure 12) The emissions are constants in time, except for some slight variation in the peaks of OH and N<sub>2</sub>. For each chemical species, its series of spectral emission and its respective electronic transitions, are collected in a table attached in the Appendix 1.

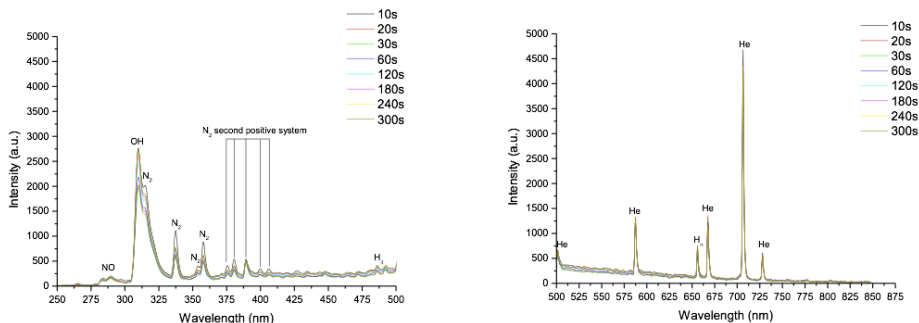


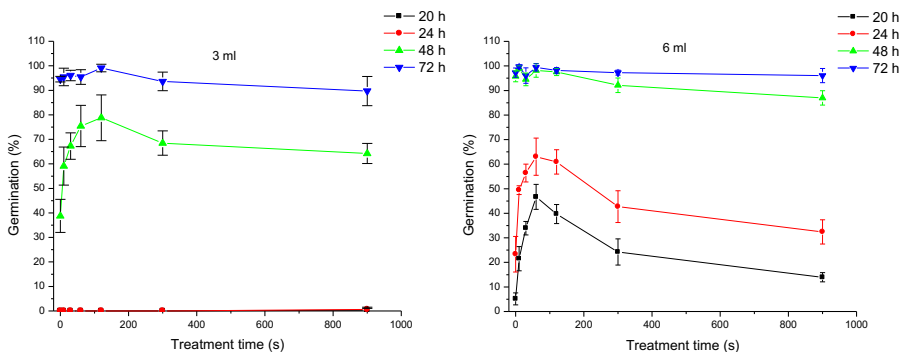
Figure 13. Optical Emission Spectroscopy spectrum of the He/air plasma and seeds.

In Figure 13, it can be observed the same plasma emissions with the seeds inside the reactor. The spectrum indicates the species of NO, OH, SPS ( $N_2$ ), H and He whereas the O emissions and FNS ( $N_2^+$ ) are not observed. In the same way as in the previous spectra, the emissions are constants in time, except for the OH and the  $N_2$ .

The decrease in intensity peaks is probably resulting from the introduction of a dielectric, such as seeds. They hinder the passage of the electric current between the electrodes and as a consequence the excitations are reduced. The peaks of FNS ( $N_2^+$ ) are not observed because it is not a majority emission and the signal is practically indiscernible. On the other hand, the disappearance of the monoatomic oxygen radicals suggests that in the presence of water in the plasma, it undergoes a quenching process, in which it reacts with water to form hydroxides. It should be noted that the differences between the peaks of OH emissions, it could be due to the water desorption of both the reactor walls and the inside of the seed and it could be for be the quenching product. The emission of  $O_2$  (762.0 nm) is not observed in the plasma.<sup>33</sup> Possibly the plasma contains other chemical species that do not emit and therefore cannot be characterized by this technique.

## 7. GERMINATION AND ABSORPTION RESULTS

The percentages of germination and absorption as function of the time of plasma treatment are shown below.





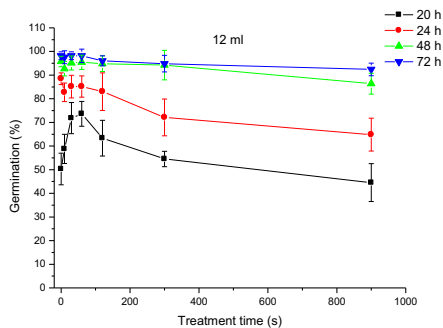


Figure 14. Percentages of germination as a function of treatment time with plasma under irrigation conditions of 3 ml, 6 ml and 12 ml.

As can be seen (Figure 14), germination depends mainly on the irrigation condition. In dry conditions (3 ml) germination starts at 48 h, while in optimal and humid conditions, germination starts at 20 h (6 ml and 12 ml, respectively). Germination according to the treatment time has a similar tendency for the three irrigation conditions. At short times ( $< 120$  s), the speed germination is greater than the untreated, while at long times ( $> 300$  s) germination is slows down. At 72 h, the final germination values are equalized for all treatment times.

After the results obtained in germination, suggesting a change in hydrophilicity of the seeds' surface, the contact angles have been measured.

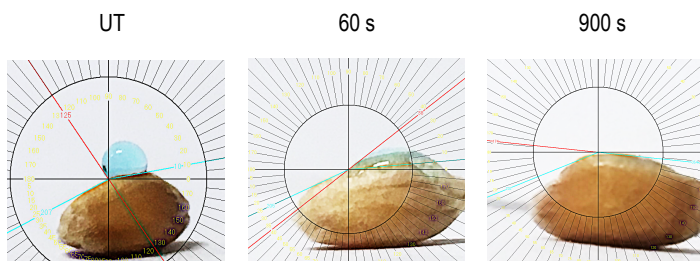


Figure 15. Measurement of contact angle of the blue methylene - seed surface treated with plasma.

It is observed that the contact angle decreases as function of the treatment time, being for the untreated higher than  $120^\circ$ , for the 60 s approximately  $30^\circ$  and for the 900 s,  $0^\circ$ . (Figure 15) Keeping the drop on the samples treated 900 s is practically impossible because the seed becomes completely wettable. However, the measurements are qualitative because there are

significant differences in the surface roughness on each sample. This experiment suggests that the surface energy of the seeds has increased promoted by the effect of plasma. This could be due to the presence of polar functional groups, which would cause the hydrophilic properties observed in the samples.

Then, the study of the absorption was carried out and the following results were obtained.

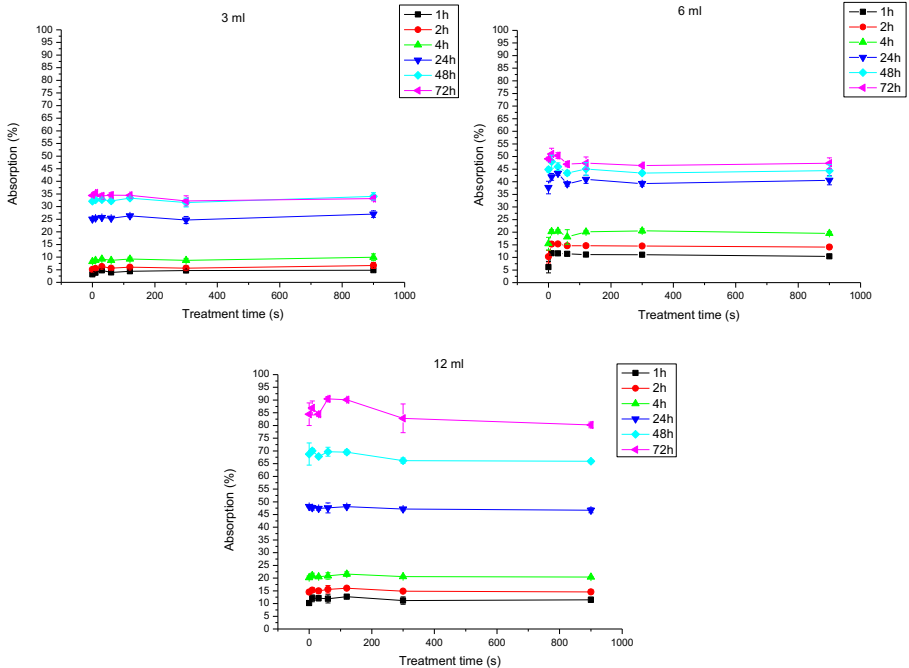


Figure 16. Percentages of absorption as a function of treatment time with plasma under irrigation conditions of 3 ml, 6 ml and 12 ml.

The weight loss is about 1% during the treatment. In dry conditions (3 ml) show a very similar absorption for all treatment times, for optimal conditions (6 ml), an increase in absorption in short times of treatment is observed and for wet conditions (12 ml) an increase in absorption is also observed for short times treatment and a slight slowing down of absorption is observed for long times of treatment. (Figure 16) It should be noted that for 6 ml and 12 ml germination starts at 20 h (Figure 14), therefore from 24 hours of absorption the values are not truthful. These results indicate that the plasma treatments favor the absorption of the water and, therefore, the germination. This fact points to the improvement of the hydrophilicity cereal surface. The slowing

down of absorption at long times of treatment under optimal and humid irrigation conditions, it suggests that water absorption hinders the exchange of gases ( $O_2$  and  $CO_2$ ) with the medium<sup>29</sup>. Weight loss during the treatment could be caused by water desorption from the inside of the seeds. It can be supposed that the effect of the plasma does not produce any damage to the embryo of the seed since the final germination (approximately with the 72h) is equalized for all treatment times. This allows the DBD plasma to be suggested as a future alternative to pre-germinative treatments, explained in the introduction.

## 8. SURFACE CHARACTERIZATION OF SEEDS

It was decided to characterize the surface of the wheat seeds after observing important changes in their germination and absorption. On the one hand, the chemical composition of the surface has been analyzed, qualitatively by the contact angle and quantitatively by XPS and FTIR-ATR techniques. On the other hand, surface topography has been examined by SEM.

By the SEM technique, the topography of the sample surface is studied.

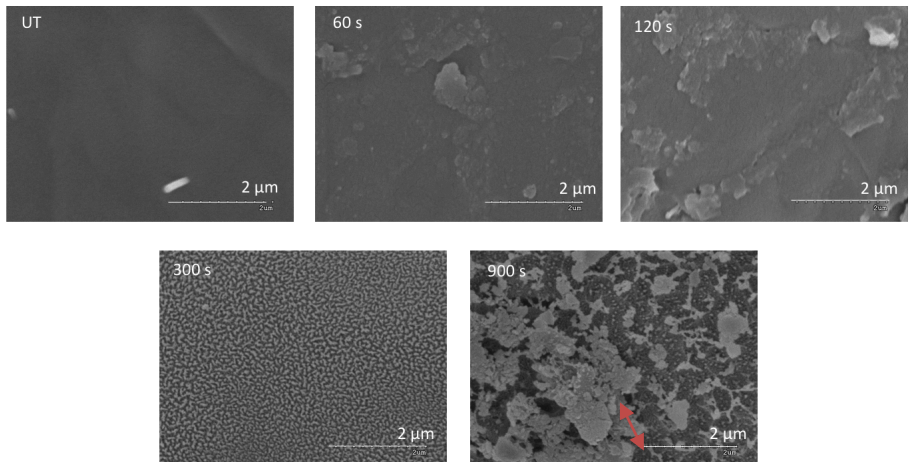


Figure 17. Images of the seed surface treated at 20x magnifications.

It is intuited a progressive degradation of the outer layer is observed as a function of the treatment time. (Figure 17) From 300 s, the damage is more noticeable. This suggests the possibility that the plasma has induced an etching effect on the surface, producing erosion of the outer layers. It cannot be insured by SEM, if the total elimination of any of the layers has occurred during the treatment. Since the thickness and chemical composition of the eroded areas is unknown (red signal).

In order to study the chemical composition of the outer layers, the FTIR-ATR technique has been used.

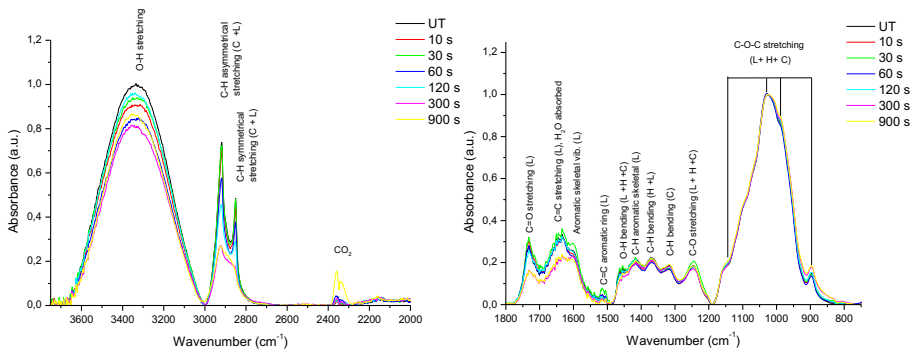


Figure 18. FTIR-ATR spectrum. L is lignin, H is hemicellulose and C is cellulose.

As spectrum describes the principal chemical composition is lignin, cellulose and hemicellulose. This mixture is characteristic of the pericarp, the outer layer of the seed. (Figure 5). It is observed that in short times the bands practically do not change. In contrast, to long times (> 300 s) are observed important changes especially in the stretching C-H ( $2928\text{ cm}^{-1}$  and  $2851\text{ cm}^{-1}$ ), in the stretching C = O ( $1735\text{ cm}^{-1}$ ) and in the bands of the benzene aromatic of the lignin ( $1641\text{ cm}^{-1}$ ,  $1610\text{ cm}^{-1}$ ,  $1510\text{ cm}^{-1}$ ). It is also observed variations in the peaks referents to O-H ( $3414\text{ cm}^{-1}$  and  $1457\text{ cm}^{-1}$ ). (Figure 18) Variations of O-H bands, gradually decrease as a time function, probably due to water desorption. These spectra suggest that at times greater than 300 s the proportion of lignin decreases considerably with respect to the rest of compounds, signifying a possible layer change due to etching induced by plasma.

Although the plasma is not thermal, there may be areas where more energy is concentrated because the conduction is not entirely homogeneous. Sometimes, the plasmas forms arcs discharge (filamentous plasmas), and the temperature can increase slightly at some points of the sample. To reject the possibility that the modification in the seed is only by the thermal effect, measurements are made for a comparison an untreated seed, one treated with plasma during 900 s and one treated at 130°C for one hour.

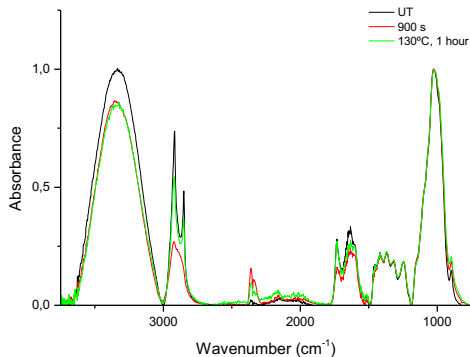


Figure 19. FTIR-ATR spectrum. Comparison of thermal treatment with plasma.

It can be seen in the green spectrum, the peaks  $3414\text{ cm}^{-1}$ ,  $2941\text{ cm}^{-1}$ ,  $2851\text{ cm}^{-1}$  and  $1641\text{ cm}^{-1}$ , decrease by thermal effect. Whereas, in the red spectrum, the peak  $1735\text{ cm}^{-1}$  is reduced, due only to the plasma effect. (Figure 19) According to the literature, hemicellulose is the only compound, of those previously named, capable of being degraded to  $130\text{ }^{\circ}\text{C}$ .<sup>38</sup> It is confirmed that the bands that have decreased due to thermal treatment belong to the hemicellulose, while the band  $1735\text{ cm}^{-1}$  (Stretching  $\text{C} = \text{O}$ ) only present in the lignin, is not modified. All bands are assigned in the table attached in Appendix 2.

This technique allows us to know if etching has been produced indirectly since we cannot characterize the modified surface. Because of the limited depth sensitivity of ATR-FTIR (Table 2), crucial information is lost from the uppermost layers, which is particularly important in case of plasma surface modification as non-thermal plasmas are known to primarily influence the first 50 nm of the sample. In contrast, XPS analyses only the first nanometers of a material surface, making it a very suitable technique to track plasma-induced surface changes. Therefore, the

changes in the surface chemical composition of the seed substrates were also studied by XPS in this work.

Previously, surveys are carried out and emissions are observed in the  $O_{KLL}$  (electrons Auger),  $O_{1s}$ ,  $N_{1s}$ ,  $C_{1s}$ ,  $K_{2p}$  and  $O_{2s}$  zones. Then, high-resolution measurements were made for the most intense peaks.

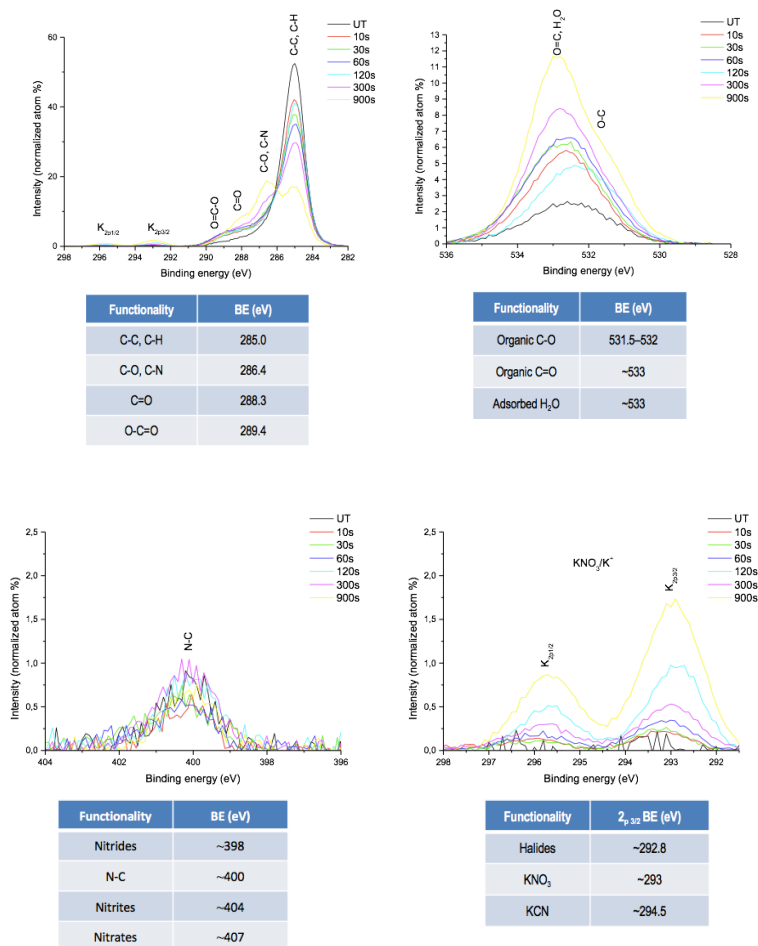


Figure 20. High resolution XPS Spectrum in the binding energy range of  $O_{1s}$ ,  $N_{1s}$ ,  $C_{1s}$  and  $K_{2p}$ .

Treatment time	%C <sub>1s</sub>	%O <sub>1s</sub>	%N <sub>1s</sub>	%K <sub>2p</sub>
UT	91,26	7,28	1,47	0
10 s	84,24	14,23	0,97	0,56
30 s	81,40	16,70	1,35	0,55
60 s	80,13	17,79	1,24	0,84
120 s	82,73	13,45	1,65	2,17
300 s	75,64	21,13	1,88	1,35
900 s	65,57	28,99	1,29	4,15

Table 3. Percentage of chemical elemental surface composition.

The percentages of photoemissions from the atoms of C, O, N and K are indicated in the Table 3. The untreated sample indicates that there are more than 90% of C<sub>1s</sub>, mostly linked as C-C and/or C-H. As can be seen, the percentage of O<sub>1s</sub> increases as function of the treatment time. At the same time, the photoemissions of C<sub>1s</sub> are progressively increasing in energy, which indicates that the electrons of carbon are more attracted. The C-C or/and C-H become to C-O, C=O and O-C=O, in this order. The difference in the ratio of O/C is more noticeable from the 300 s of treatment. On the other hand, the percentage of K<sub>2p</sub> increases and the N<sub>1s</sub> remains practically constant.

After the results of the untreated sample, it indicates the existence of a possible layer, composed of hydrocarbon chains that would cover the pericarp. This layer has not been found in the literature, but other experiments have obtained similar results for Quinoa.<sup>29</sup> This layer could have an apolar composition and give the hydrophobic character to the surface of the seed. The appearance of K<sub>2p</sub>, it can be attributed to potassium salts diffused to the outermost layers due to the desorption of H<sub>2</sub>O during the treatment. Thanks to the increase of O<sub>1s</sub>, a progressive oxidation of the possible hydrocarbon layer is intuited. According to the literature, the ratio of O/C of the lignin is 0, 35,<sup>39</sup> to 900 s, in which the ratio O/C is 0.43, it can indicate that the plasma has induced the etching. It could be mean that the hydrocarbon chain is eliminated by letting partially see the lignocellulosic composition of the pericarp.

After the study of chemical species that contains the plasma and the effect that induces on the seed surface, the suggested etching mechanism is as follows.<sup>14</sup>

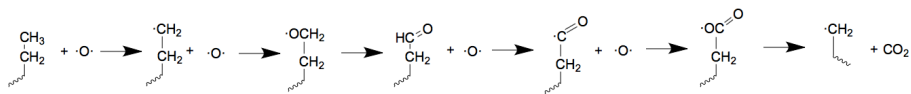


Figure 21. Etching mechanism of a hydrocarbon chain.

The mechanism shown, initially consists of the superficial bombardment of photons, electrons, ions, atoms and excited species that form radicals on surface. The OES (Figure 13), indicated that plasma has a chemical oxidant species, such as hydroxide and monoatomic oxygen. This fact suggests that these radicals are the main reagents of the oxidations that are carried out. Then, there are consecutive oxidations as indicated in the previous XPS experiment (Figure 20). The mechanism ends with the release of volatile compounds, such as CO<sub>2</sub>. (Figure 21)

## 9. FUTURE WORKS

This project will continue to be developed with the aim of solving problems encountered during the realization of this work. For future experiments, with the objective to know the chemical elemental composition for each layer it has been proposed to make a cross-section of the seed, to perform a microanalysis in the different layers by Energy Dispersive X-ray Spectroscopy (EDXS). In addition, to know the exact dimensions of the layers is proposed to perform a controlled sputtering in different times by argon atoms' collisions, causing erosion at different depths and analysing them using XPS.



## 10. CONCLUSIONS

The OES analysis of the chemical species present in the plasma, indicates that the plasma of He has air and water impurities, such as, monoatomic radicals of oxygen, nitrogen monoxide, monoatomic hydrogen, excited species of molecular nitrogen and hydroxyl radicals.

Thanks to these chemical species, it has been possible to modify the first nanometers of the seed surface, improving its superficial properties, such as hydrophilicity, as indicated by changes in the contact angle with the surface of the seed.

The process of germination of wheat seeds has been accelerated by an improvement in water absorption after short time (< 120 s) of exposure to plasma DBD. And at long time of treatment (> 300 s) germination is slows down, especially in conditions of hydric stress (humid conditions). It is suggested that the exchange of gases ( $O_2$  and  $CO_2$ ) with the outside is hampered. At 72 h of germination is equalized for all treatment times, discarding the possibility of having damaged the embryo. The arguments given above prove that treatments with atmospheric plasma could be a future more profitable alternative and environmentally friendly than the current chemical pre-germinative treatments.

The surface characterization techniques used, physical-chemical changes induced by the plasma on the surfaces of the seeds are observed. In one hand, the chemical composition of the pericarp has been determined by the FTIR-ATR (lignin, cellulose and hemicellulose) that does not change in short times of treatments, but a lignin reduction is observed at long times. On the other hand, the XPS has shown the existence of a layer that covering the pericarp and its thickness is below the FTIR-ATR detection depth limit. The composition of this layer is greater than 90% of C-H or C-C, it suggested could be hydrocarbon chains that award the hydrophobia to the surface of the seed.

Finally, following the results of the XPS, it is concluded that a process of functionalization is induced by plasma because it indicates the oxidation of the layer (incorporating polar functional

groups on the surface that increase the hydrophilia). In contrast, from the 300 s of treatment, with the SEM there is an important degradation in the outer layer with the FTIR-ATR is determined a change in the chemical composition and with the XPS an increase in the ratio O/C more noticeable. From the above, it has been concluded that occurs the partial or total elimination of the hydrocarbon layer meaning an etching process induced by plasma.

## 11. REFERENCES AND NOTES

1. Wolf, Rory A.; *Atmospheric Pressure Plasma for Surface Modification*; John Wiley and Sons, 2012; pp. 205-221.
2. Dinklage, A.; Klinger, T.; *Plasma Physics*; Springer Science & Business Media, 1998; p. 57.
3. Twedt, K. A.; Rolston, S.L.; Electronic Detection of Collective Modes of an Ultracold Plasma. *Phys. Rev. Lett.*, **2012**.
4. Langmuir, I.; Oscillations in ionized gases; *Proc. Nat. Acad. Sci. U.S.*, vol. 14, p. 628, **1985**.
5. Kalinowski, J; Excimers and Exciplexes in Organic Electroluminescence; *Materials Science-Poland*, **2009**.
6. Wang, Y.; C. Li, J. SHI, X. WU, and H. DING; Measurement of Electron Density and Electron Temperature of a Cascaded Arc Plasma Using Laser Thomson Scattering Compared to an Optical Emission Spectroscopic Approach; *Plasma Sci. Technol.*, Vol. 19, **2017**.
7. Schutze, A.; Jeong, J.; Babayan, S.; The Atmospheric-Pressure Plasma Jet: A Review and Comparison to Other Plasma Sources; *IEEE Trans. Plasma Sci.*, Vol. 26, 6, **1998**, pp. 1685-94.
9. Klämpfl, T; Cold Atmospheric Plasma Decontamination Against Nosocomial Bacteria; Universität München, **2014**, pp. 10-20.
10. Hossain, M. M; *Plasma Technology for Deposition and Surface Modification*. Logos Verlag Berlin GmbH, **2009**, p. 86.
11. Liston, E.; Martinu L.; Wertheimer, M.; Plasma Surface Modification of Polymers for Improved Adhesion: A Critical Review. *Jour. Adh. Sci. Techn.*, Vol. 7, 10, **2012**, pp. 1091-27.
12. Diener electronics; <https://www.plasma.com/en/applications/plasma-etching/> (Accessed 10 Abr., 2019)
13. D. M. Mattox, in Handbook of Physical Vapor Deposition (PVD) Processing (Elsevier, 2009), pp. 343–405.
14. Moss, S.; Jolly, A.; Tigue, B.; Plasma Oxidation of Polymers. *Plasma Chemistry and Plasma Processing*, Vol. 6, **1986**, pp. 401-15
15. Electronic Spectroscopy [http://www.phys.ubbcluj.ro/~dana.maniu/OS/BS\\_6.pdf](http://www.phys.ubbcluj.ro/~dana.maniu/OS/BS_6.pdf) (Accessed 16 Abr., 2019)
16. Río, L. A.; ROS and RNS in Plant Physiology: An Overview; Vol. 66, 10, **2015**, pp. 2827-3.
17. Ho, R. Y. N.; Liebman, J. F.; Valentine, J. S.; Overview of Energetics and Reactivity of Oxygen. Active Oxygen in Chemistry. *Chapman and Hall, Bishopbriggs*, Glasgow, UK, **1995**, pp. 1 - 23.
18. Sivachandiran, L.; Khacef, A.; Enhanced Seed Germination and Plant Growth by Atmospheric Pressure Cold Air Plasma: Combined Effect of Seed and Water Treatment. *RSC Adv.*, Vol. 7, 4, **2017**, pp. 1822-3.
19. Cardinaud, C.; Fluorine-Based Plasmas: Main Features and Application in Micro-and Nanotechnology and in Surface Treatment; *Comptes Rendus Chimie*, Vol. 21, 8, **2018**, pp. 723-39.
20. Latencia y germinación de semillas. Tratamientos pregerminativos; [https://inta.gov.ar/sites/default/files/script-tmp-inta\\_latencia.pdf](https://inta.gov.ar/sites/default/files/script-tmp-inta_latencia.pdf) (Accessed 16 Abr., 2019)

21. Knudsen, K. E. B. Fiber and Nonstarch Polysaccharide Content and Variation in Common Crops Used in Broiler Diets. Vol. 93, no. 9, **2014**, pp. 2380-93.
22. The regional institute <http://www.regional.org.au/au/cereals/2/12stone.htm> (Accessed 17 Abr., 2019)
23. Sivachandiran, L.; Khacef, A.; Enhanced Seed Germination and Plant Growth by Atmospheric Pressure Cold Air Plasma: Combined Effect of Seed and Water Treatment. *RSC Adv.*, Vol. 7, 4, **2017**, pp. 1822-3.
24. Walzak, M.; Davidson, R.; Biesinger, M.; The Use of XPS, FTIR, SEM/EDX, Contact Angle, and AFM in the Characterization of Coatings. Vol. 7, 3, **1998**, pp. 317-23.
25. Rodríguez, A.; Estudio Del ángulo De Contacto Y De La Mojabilidad a Alta Temperatura De Fases Líquidas En La sinterización De Metales. Universidad Carlos III; Madrid, 1, 2010.
26. Interacción de los electrones con la material; <https://ssyf.ua.es/es/formacion/documentos/cursos-programados/2012/especifica/tecnicas-instrumentales-en-el-analisis-de-superficie/sem-sesion-12-de-noviembre.pdf>; Serveis Tècnics d'investigació; 2012. (Accessed 21 May,2019).
27. FT-IR Spectroscopy Attenuated Total Reflectance (ATR). *PerkinElmer* (Accessed 21 May,2019).
28. Moulder, J. F. *Handbook of X Ray Photoelectron Spectroscopy*. 1995.
29. Molina, R.; López-Santos, C; Gómez-Ramírez, A.; Vilchez, C.; Espinós, J.P.; González-Elipe, A.R.; Influence of Irrigation Conditions in the Germination of Plasma Treated Nasturtium Seeds. *Sci Rep*, Vol. 8, 1, **2018**.
30. Matilainen, A.; Britun, N.; Bong, J.S.; Optical Emission Spectra of OMCTS/O<sub>2</sub> Fed Plasmas Used for Thin Film Deposition; *Surface and Coatings Technology*, Vol. 205, **2010**, pp. 300-4.
31. Milosavljević, V.; Donegan, M.; Cullen, P.J.; Diagnostics of an O<sub>2</sub>-He RF Atmospheric Plasma Discharge by Spectral Emission; *J. Phys. Soc. Jpn.*, Vol. 83, 1, **2014**.
32. Rezaei, F.; Nikiforov, A.; Morent, R.; Plasma Modification of Poly Lactic Acid Solutions to Generate High Quality Electrospun PLA Nanofibers; *Sci Rep*, Vol. 8, 1, **2018**.
33. Bourig, A.; Lago V.; Martin, J.P.; Generation of Singlet Oxygen in HV Pulsed + DC Crossed Discharge at Atmospheric Pressure for Oxygen-Enhanced Combustion. *International Journal of Plasma Environmental Science & Technology*, 1, **2007**, pp. 57-63.
34. Abidi, N.; Cabrales, L.; Haigler, C.H.; Changes in the Cell Wall and Cellulose Content of Developing Cotton Fibers Investigated by FTIR Spectroscopy; *Carbohydrate Polymers*, Vol. 100, **2014**, pp. 9-16.
35. Yang, H.; Yan, R.; Chen, H.; Characteristics of Hemicellulose, Cellulose and Lignin Pyrolysis; *Fuel*, Vol. 86, 12-13, **2007**, pp. 1781-8.
36. Ganne-Chédeville, C.; Jääskeläinen, A.S.; Froidevaux, J.; Natural and Artificial Ageing of Spruce Wood As Observed by FTIR-ATR and UVR Spectroscopy. Vol. 66, 2, **2012**.
37. Bilba, K.; Ouensanga, A.; Fourier Transform Infrared Spectroscopic Study of Thermal Degradation of Sugar Cane Bagasse. *Journal of Analytical and Applied Pyrolysis*, Vol. 38, 1-2, **1996**, pp. 61-73.
38. Carrasco, M.; Bueno, A.; OBTENCIÓN Y CARACTERIZACIÓN FÍSICOQUÍMICA Y FUNCIONAL DE LAS FIBRAS DIETÉTICAS DEL NÍSPERO COMÚN (*Mespilus Germanica*) a a B OBTENTION, FUNCTIONAL AND PHYSICO-CHEMICAL CHARACTERIZATION OF THE DIETARY FIBERS OF COMMON MEDLAR (*Mespilus Germanica*); *Rev Soc Quím Perú*, Vol. 74, no. 4, Jan. **2008**.
39. Rinaldi, R.; Woodward, R.; Ferrini, P.; Lignin-First Biorefining of Lignocellulose: The Impact of Process Severity on the Uniformity of Lignin Oil Composition; *J. Braz. Chem. Soc.*, **2018**.

# APPENDICES



## APPENDIX 1: OES

Species	Peaks Assignment (nm)	Electronic transition	Bibliography
<b>OH</b>	309,0	$A^2\Sigma^+ - X^2\Pi$	30,31
<b>CO</b>	662,0; 607,9; 561,0; 519,8; 483,5; 451,1; 439,3	Angstrom System $B^1\Sigma^+ - A^1\Pi$	30
<b>N<sub>2</sub></b>	399,8; 380,4; 375,5; 357,5; 337,1	Second Positive System (SPS) $C^3\Pi - B^3\Pi$	32
<b>N<sub>2</sub><sup>+</sup></b>	470,9; 427,8; 423,7	First Negative System (FNS) $B^2\Sigma^+_u - X^2\Sigma^+_g$	32
<b>He (S=1)</b>	501 667 728	$2s^1S_0 - 3p^1P_1$ $2p^1P_1 - 3d^1D_2$ $2p^1P_1 - 3s^1S_0$	31
<b>He (S=3)</b>	388 587 706	$2s^3S_1 - 3p^3P_{0,1,2}$ $2p^3P_{0,1,2} - 3d^3D_{1,2,3}$ $2p^3P_{0,1,2} - 3s^3S_1$	31
<b>H</b>	H <sub>α</sub> 656,3 (red) H <sub>β</sub> 486,1 (green) H <sub>γ</sub> 431,1 (violet)	Balmer line $n=3 - n=2$ $n=4 - n=2$ $n=5 - n=2$	30,31
<b>O (S=3)</b>	845	$3s^3S_1 - 3p^3P_{0,1,2}$	
<b>O (S=5)</b>	615 777	$3p^5P_{1,2,3} - 4d^5D_{0,1,2,3,4}$ $3s^5S_2 - 3p^5P_{1,2,3}$	30
<b>NO</b>	380,1; 358,3; 338,6; 320,7; 304,3; 289,3; 275,4	$\beta$ System $B^2\Sigma^+ - X^2\Pi$	32

## APPENDIX 2: FTIR-ATR

Wavenumber (cm <sup>-1</sup> )	Band assignment	Hemicellulose	Cellulose	Lignin	Bibliography
3414-3423	Stretching O-H	x	x	x	34
2928-2937	Asymmetrical Stretching C-H		x	x	34,35
2851	Symmetrical Stretching C-H		x	x	34,35
1735	Stretching C=O	x			34,36
1641	Absorbed H <sub>2</sub> O				34
1601	Aromatic skeletal vibration			x	36
1506-1510	Aromatic skeletal vibration			x	36
1457-1459	Bending C-H	x	x	x	36
1423	Aromatic skeletal C-H			x	36
1382	Bending C-H	x	x	x	37
1365	Bending C-H	x	x		36,37
1328	Bending C-H		x		31
1219-1269	Stretching C-O	x	x	x	32,33
1117-1215	Anti-symmetrical stretching C-O	x	x		32,33
1031-1036	Bending C-O-C	x	x	x	32
836-867	Bending out of plane C-H		$\beta$ -linkage <sup>30</sup>	x	30



